Nanostructured V_2O_5 thin films prepared spray pyrolysis technique for NO_2 sensor

J. M. Patil*[1], S. B. Patil[2] R. H. Bari[2], and A. N. Sonar[1]

[1]*Department of Chemistry, Shri. V. S. Naik, A.C.S. College, Raver, 425508, Maharashtra, India.
[2]Nanomaterials Research Laboratory, Department of Physics, G. D. M. Arts, K. R. N. Com. And M. D. Science College, Jamner, 424 206, Maharashtra, India.

Abstract: Nanostructured thin films of V_2O_5 are sensitive to change in their environment. V_2O_5 is successfully used as gas sensor due to the dependence of the electrical conductivity on the ambient gas composition. Nanostructured V_2O_5 thin films of different spray deposition time (5 min., 10 min., and 15 min.,) were deposited onto heated glass substrate at 350 $^{\circ}$C by simple spray pyrolysis (SP) technique. Sensing elements of nonostructured V_2O_5 were annealed at 500 $^{\circ}$C for 60 min. Characterization includes a different analytical technique such as, X-ray diffaractogram (XRD), energy dispersive X-ray analysis (EDAX), and Field emission scanning electron microscope (FE-SEM). The average grain size observed from XRD and FF-SEM was found to be less than 24 and length of the rod 370 nm respectively. The films sprayed for 10 min. was observed to be most sensitive (S = 531) to NO_2 for 500 ppm at 350 $^{\circ}$C. The response and recovery time is 2 sec, 11 sec respectively.

Keywords: Spray Pyrolysis, Nanostructured V_2O_5, NO_2 gas sensing, quick response, fast recovery.

1. Introduction

Recently nanostructured metal-oxides have attracted much attention because of their potential applications in gas sensors. Nanostructured metal-oxides provide high surface to volume ratio, while maintaining good chemical and thermal stabilities with minimal power consumption and low weight. Nanostructures used in the fabrication of gas sensors include metal-oxides in the form of nanorods [1] nanowires [2], and nanobers [3]. Research and development of gas-sensing devices is in the focus of activity of scientists and engineers in many countries. Gas sensors can be manufactured using different materials, technologies and phenomena. Sensing devices should be smaller and cheaper hence research regarding sensitivity, selectivity, response-recovery time, reproducibility, cost, portability, deposition techniques, fabrication of devises, operating temperatures and gas concentration for different materials and gases is necessary [4]. Metal oxide semiconductor (MOS) sensor technology is based on the change in resistance of a sensitive metal oxide layer which is induced by the interaction between a surface and ambient gases. Metal oxide semiconductors demonstrate good detection sensitivity, robustness and the ability to withstand high temperatures and the technique is commonly used to monitor a variety of toxic and inflammable gases in a variety of air pollution monitoring systems, the food industry, medical diagnosis equipment and gas leak alarms. Since the last decade there has been a great deal of interest in the preparation of inexpensive thin films of nanostructures V_2O_5. This is because V_2O_5 based thin films with large band gap (Eg>3eV) n-type semiconductors are attractive from the scientific and technological point of view [5-8].

Vanadium exists in a number of oxide forms, the di-, sesqui- and pentoxides (VO_2, V_2O_3 and V_2O_5).

They have been processed in thin film form and applied as optical and electrical devices. Especially vanadium oxide (V_2O_5), as a wide band gap and n-type semiconductor material, was widely investigated because of its interesting electrochemical performance. Vanadium oxide-based materials including vanadium pentoxide, vanadium phosphates can be used as catalysts for the mild oxidation of hydrocarbons and alcohols [9]. During the last years, an increasing interest has been devoted to hybrid vanadium oxides due to their potential application as catalysts, sensors, electrodes.

In order to improve the properties of the films, sevaral techniques have been employed to prepare vanadium pentaoxide (V_2O_5) thin films. These include template-assisted growth based on electro deposition [10], surfactant/inorganic self-assembly [11], e-beam sputtering, chemical-vapor deposition [12] and pulsed laser deposition [13] and spin-coating [14] methods. Among these techniques, spray pyrolysis has proved to be simple, reproducible and inexpensive, As well as suitable for large area applications. Besides the simple experimental arrangement, high growth rate and mass production capability for large area coatings make them useful for industrial as well as solar cell application. In addition, spray pyrolysis opens up the possibility to control the film morphology and particle size in the nm range.

The aim of this work is to present a structural, microstructure and electrical properties study of nanostructured V_2O_5 thin films prepared by spray pyrolysis method and demonstrates for sensing different gases and were observed to be most sensitive to NO_2 at 350 ^{O}C. Phase purity and grain sizes were examined using X-ray diffraction, Field emission scanning electron microscope (FESEM). The effect of spraying time of the solution on structural, surface morphology, and gas sensing properties were studied and investigated.

2. Experimental details

2.1. Substrate Cleaning

The substrate cleaning is very important in the deposition of thin films. Commercially available glass slides with a size of 25 mm×25 mm×1 mm were washed using soap solution and subsequently kept in hot chromic acid and then cleaned with deionized water followed by rinsing in acetone. Finally, the substrates were previously cleaned with deionized water for 20 min and wiped with acetone and stored in a hot oven.

2.2. Preparation of nanostructured V_2O_5 thin films

Figure 1 shows spray pyrolysis technique for preparation of nanostructured V_2O_5 thin films. Set-up consists of spraying chamber, spray nozzle (gun), compressor for carrier gas, heating system, and temperature indicator.
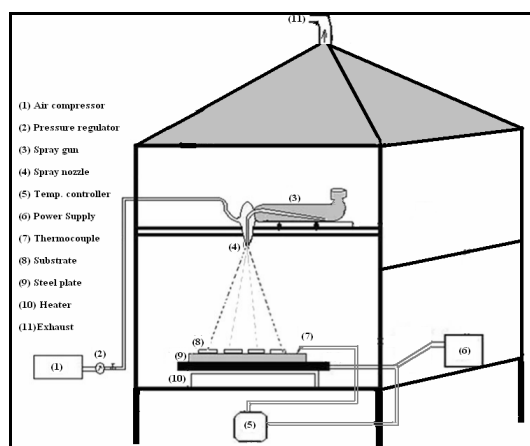

(1) Air compressor
(2) Pressure regulator
(3) Spray gun
(4) Spray nozzle
(5) Temp. controller
(6) Power Supply
(7) Thermocouple
(8) Substrate
(9) Steel plate
(10) Heater
(11) Exhaust

Figure1. Schematic diagram of spray pyrolysis system for the preparation of nanostructured V_2O_5 thin films.

V_2O_5 thin films were prepared by using Vanadium (III) chloride (VCl_3), Purified Aldrich) in de-ionized water as a precursor. A concentration of precursor solution (0.05M) was sprayed through a specially designed glass nozzle of 0.5 mm inner diameter onto the ultrasonically cleaned glass substrates. Then solution was sprayed at the following conditions: carrier-air pressure: 1-2 atm, flow rate of solution: 9 ml/min, substrate

temperature: 350 °C, spray time interval (5 min., 10 min., 15 min.) and substrate to nozzle distance: 30 cm. as prepared nanostructured V_2O_5 samples referred as S1, S2, and S3. For preventing reduction at hot plate temperature, spraying was done in short time intervals. The metallic salt solution, when sprayed onto a hot substrate, pyrolitically decomposes and a chemical reaction takes place on the heated substrate and at least a thin layer of V_2O_5 is deposited.

Thin films were annealed in a Muffle furnace at 500 °C for 60 minutes. This was done in order to improve the microstructure and crystallization of the thin films. Apart from crystallization and microstructure improvement, annealing was done in order to improve the gas sensing properties of the thin films.

2.3. Kinetics in thin film deposition

The deposition process needs fine droplets to react on the heated substrate, owing to the pyrolytic decomposition of the solution. The hot substrate provides the thermal energy for the thermal decomposition and subsequent recombination of the constituent species. In many cases large droplets of the solution do not vaporize before reacting to deposit on the substrate. They hit the surface and form a powdery deposit. If it strikes at a high enough velocity, the droplet will splatter and form a dispersed powdery layer. As mentioned above, the droplet cannot be completely vaporized before it hits the surface and for this reason, film growth cannot occur investigated the mechanism of V_2O_5 film growth. The influence of forces which determine both the trajectory of the droplets and evaporation were examined and a film growth model was proposed. Figure 2 shows the types of trajectories that are expected to occur in the spraying of a solution on hot glass substrate. It is reported that the behaviour of precursor drops undergo three major steps during the course of spray pyrolysis: (i)drop size shrinkage due to evaporation, (ii) conversion of precursor into oxides, and (iii) solid particle formation. The particle formation may involve two mechanisms: intraparticle reaction (conventional one-particle-per-drop mechanism) and gas-to-particle conversion [15].
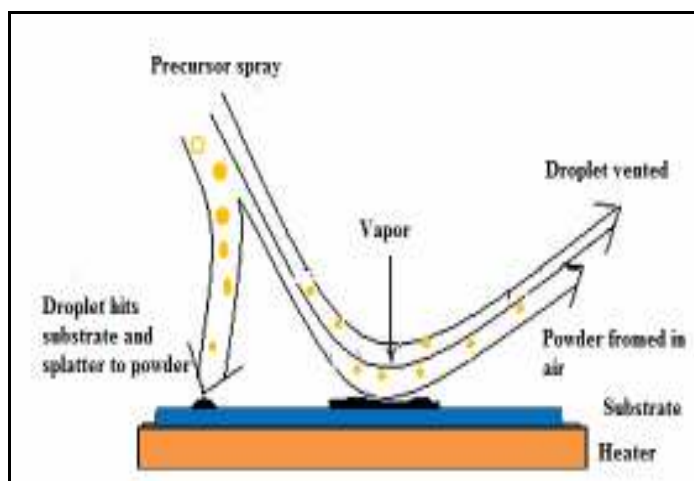

Figure 2. Kinetics in thin film deposition

In the one-particle-per-drop mechanism, each droplet is regarded as a micro reactor and converts into one solid particle when it travels towards substrate. In contrast, gastoparticle conversion occurs when the precursor is volatile and is transported across the particle–gas interface.

The phenomenon for the preparation of a metal oxide thin film depends on surface hydrolysis of metal chloride on a heated substrate surface in accordance with the equation,

$XClm + nH2O \rightarrow XOn + mHCl$-----------------(1)
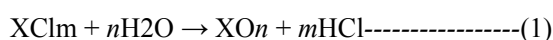
Where X is the metal such as V, Sn, Zn, Cu etc of the oxide films.

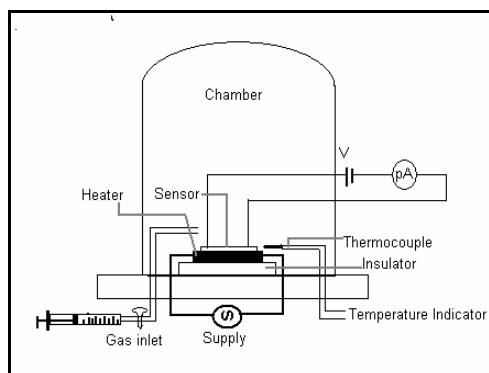**2.4. Sensing system to test the sensor**

Figure 3. Schematic diagram of static gas system

The sensing characteristics of nanostructured V_2O_5 thin film sample were obtained with a home built apparatus consisting of a temperature controller, a chromel-alumel thermocouple, an electric heating plate, a gas chamber and picoammeter as shown in Figure 3.

For electrical measurements, silver contacts (3mm X 3mm) were used to form ohmic contacts on the samples. After placing a fabricated sensor in the test assembly, a known quantity of

LPG, carbon dioxide, carbon monoxide, hydrogen, ammonia, ethanol, NO_2, and chlorine was injected into the test chamber at suitable temperature from 200 ^{0}C to 400 ^{0}C and variation of resistance of a sensor was monitored and recorded. The conductance of sensor element was calculated by equation (2)

$$S = \text{———} \qquad \text{…………… (2)}$$

Where, Gg and Ga are the conductance in the presence of test gas and in air respectively.

2.5. Thin film characterizations

The nanostructured V_2O_5 thin film were characterized by X-ray diffraction (Miniflex Model, Rigaku, Japan) using CuKα radiation with a wavelength, $\lambda = 1\cdot5418$ Å. The microstructure of the films was analyzed using a field emission scanning electron microscope (FE-SEM, JEOL. JED 6300). Electrical and gas sensing properties were measured using a static gas sensing system. The sensor performances were measured on exposure of LPG, carbon dioxide, carbon monoxide, hydrogen, ammonia, ethanol, NO_2, and chlorine was tested.

3. Results and discussion

3.1. X-ray diffraction analysis

Figure 4(a), (b) and (c) shows the X-ray diffractogram of thin film samples S1, S2, and S3. The peaks (200), (110), (400), (002), (220), (311), (112), (331), and (004) in the XRD pattern are match well with the ASTM data book of pure V_2O_5 [16]. These diffraction profiles illustrate crystalline nature and monoclinic phase of V_2O_5 thin films.
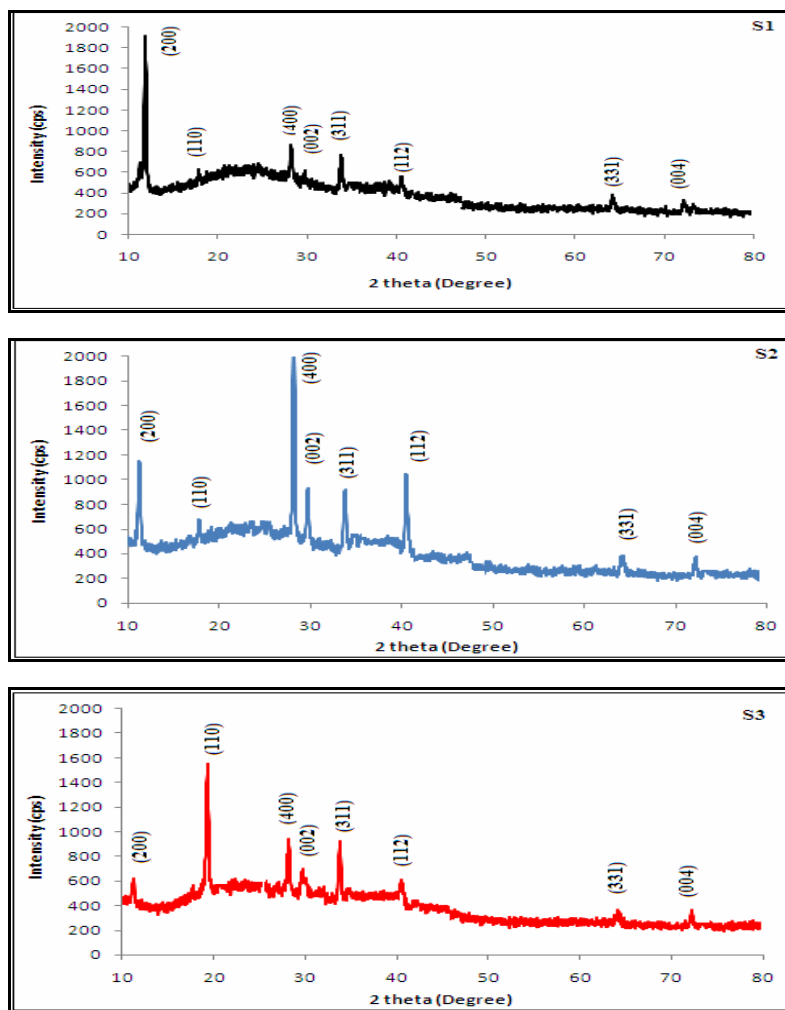
Figure 4. X-ray diffractogram of nanostructured V_2O_5 thin films samples: (a) S1, (b) S2, and (c) S3.

In XRD pattern, (200) peak has the most distinct reflection. By employing Debye-Scherrer equation for the X-ray diffaractogram (XRD) peaks the average grain size was found to be few nanometer. XRD of the film show their nanostructured nature with dominant orientation along (200) plane.

$$D = K \lambda / \beta \cos \theta \text{-------------- (3)}$$

Where, K is constant (0.94), λ is the wavelength of the X-ray used, β is broadening of diffraction line measured at half of its maximum intensity (in rad) and θ is Bragg's diffraction angle.

The calculated grain sizes were presented in Table 2.

3.2 Surface Morphology

The microstructure of the prepared film was analyzed using a field emission scanning electron microscope (FE-SEM, JEOL. JED 6300)

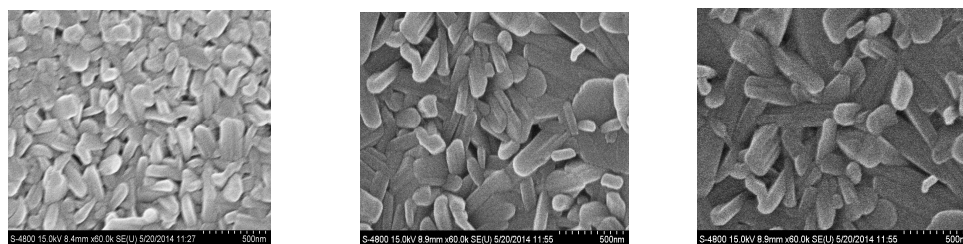 (a)   (b)   (c)
Figure 5. FESEM images: (a) S1, (b) S2, and (c) S3.

Fig. 5 (a)–(c) shows the FESEM images, showing surface morphology of S1, S2, and S3 thin film samples respectively. Field emission Scanning electron microscope (FE-SEM) show the presence of nanorod shaped. We observed that the smaller grains expand to larger grains which are referred to a nucleation stage. Surface diffusion phenomenon [17] contributes an important role in the growth process of V_2O_5 where the particles jump between adjacent sites on a surface and the motion increase with increasing thickness of the films. As prepared V_2O_5 thin films deposited on the substrate does not have enough energy to form crystalline structure due to the lower thickness. The higher thickness of the films provides thermal energy to activation of crystallization. Grain size observed to be in the range from 28 nm to 43 nm. The observed grain sizes were tabulated in Table 2.

3.3. Quantitative elemental analysis (EDAX)

The atomic compositions of the grown films have been determined by Energy Dispersive Analysis of X-ray (EDAX) method. Table 1 shows the elemental composition of the films from EDAX. Theoretically expected stoichiometric composition of V_2O_5 (in terms of at.%) is: V = 28.57%, O = 71.43.
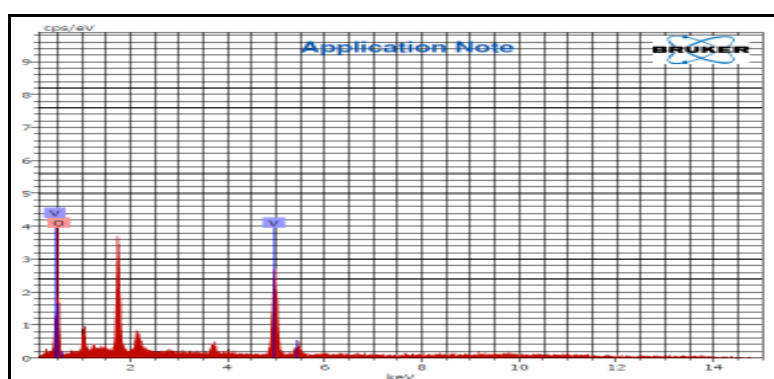

Figure 6.Elemental analysis of thin film sample (S2)

Table 1. Quantative elemental analysis as prepared nanostructured V_2O_5 thin film

Element	Stoichiometric proportion		Observed					
			Sample S1		Sample S2		Sample S	
	wt %	at %	wt %	at %	wt %	at %	wt %	at %
V_2	60.40	28.57	43.81	19.67	45.38	21.76	58.58	30.76
O_5	39.60	71.43	56.19	80.33	54.62	78.24	41.42	69.24
V_2O_5	100.00	100.00	100.00	100.00	100.00	100.00	100.00	100.00

It is clear from table 1 that the films are observed to be non-stoichiometric in nature. As the spraying time of the solution increases, the films were observed to be oxygen deficient.

3.4. Determination of film thickness

Film thickness was measured by using a weight difference method [18]. (Considering the density of the bulk V_2O_5). In order to measure the thickness of the thin films by using a weight difference method, error and accuracy was found to be ± 5 % nm. The films were deposited on clean glass slides whose mass was previously determined. After the deposition the substrate was again weighted, determining the quantity of deposited V_2O_5. Measuring the surface area of the deposited film, taking account of V_2O_5 specific weight of the film, thickness was determined using the relation:

The thickness, sample weight and sample area are related as:
$$t = M/A.\rho \text{ ----------------- (4)}$$

Where, M is the weight of the sample in *gm*, A the area of the sample in cm^2

and ρ the materials density in gm cm^{-3}.
The values of the film thickness are given in Table 2.

Table 2: Measurement of spray deposition time, film thickness, and grain size (From XRD and FE-SEM)

Sample	Spray time of solution (min.)	Thickness (nm)	Grain size from XRD (nm)	Grain size from FE-SEM (nm)
S1	5	118	19	28
S2	10	124	24	37
S3	15	139	29	42

In Table 2 the thickness of the film was varied from 118 to 139 nm. It was found that the thickness of the film increases, with increase in spray time of the solution. It is also clear from table that grain sizes are goes on increasing with increase in film thickness.

3.5. Electrical properties
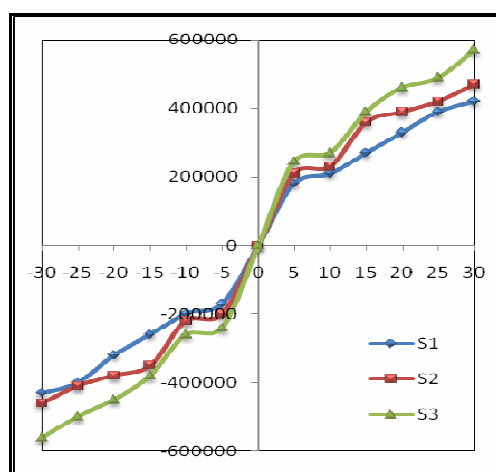
3.5.1. I–V characteristics

Figure 7. I–V characteristics of nanostructured V_2O_5 thin film sensors.

Figure 7 shows *I–V* characteristics of nanostructured V_2O_5 thin films. The graphs are observed to be symmetrical in nature indicating ohmic contact. The non-linear I–V characteristics may be due to semiconducting nature of the films.
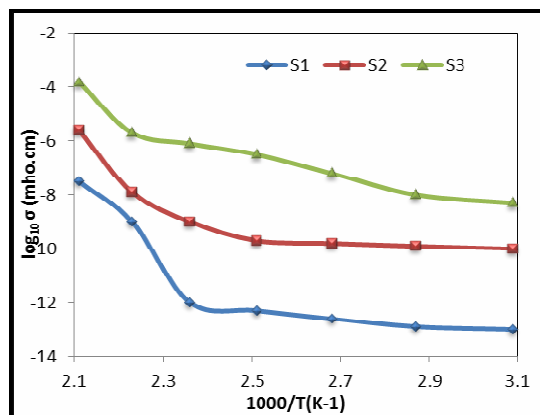
3.5.2. Electrical conductivity

Figure 8. Variation of log (conductivity) with operating temperature (∘C).

Fig. 8 show the variation of log (conductivity) with operating temperature. The conductivity of each sample is observed to be increasing with an increase in temperature. The increase in conductivity with increase in temperature could be attributed to negative temperature coefficient of resistance and semiconducting nature of nanocrystalline V_2O_5.

It clearly indicates that the nanostructured V_2O_5 thin films are semiconducting in nature. It was reported [19, 20] as thickness of the film increases activation energy goes on decreasing. In Table 3.the activation energy calculated from slopes of line for 5 min., 10 min., and 15 min. thin films were found (200-400 °C) to be 0.50 eV, 0.46 eV, 0.47 eV, 0.36 eV, 0.37 eV and 0.27 eV respectively.

Table 2: Measurement of activation energy and film thickness

Sample No.	Thickness (nm)	Activation energy($\triangle$E) eV	
		200 °C	400 °C
S1	118	0.50	0.46
S2	124	0.47	0.36
S3	139	0.37	0.27

3.6. Gas sensing performance of the sensors

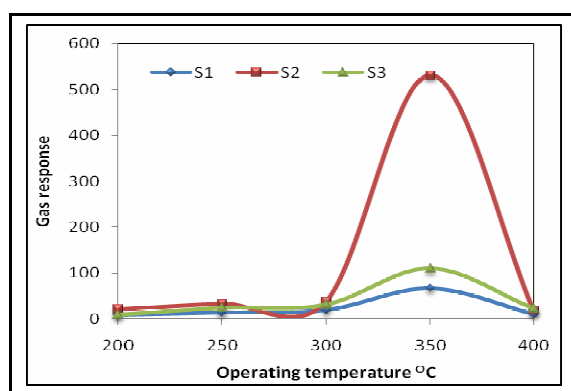**3.6.1. Effect of operating temperature on the sensor**

Figure 9. Gas response of pure nanostructured V_2O_5 thin films with operating temperature.

From Figure 9, it is found that sensitivity increases with increase in operating temperature and show maximum peak values at certain temperatures called optimal temperature and then decreases with further increase in temperature [21]. At the optimal temperature, the activation energy may be enough to complete the chemical reaction. The observed increase and decrease in the sensitivity indicates the adsorption and desorption phenomenon of the gases. The optimal temperature was confirmed for each V_2O_5 film samples for five cycles. For NO_2 gas, the response was observed to increase with operating temperature up to 350 °C. Sensor S2 is most sensitive to NO_2 at 350 °C as compared to sensors S1 and S3. After 350 °C temperature the surface would be unable to oxidize the gas so intensively and the NO_2 may expose before reaching the surface of the film at higher temperature. Thus, the gas sensitivity decreases with increasing temperature. The resistance variation in air is attributed to the effect of oxygen chemisorption. It is generally accepted that oxygen is chemi-adsorbed at a surface site such as oxygen vacancy in the form of an ionized oxygen atom or molecule, i.e. O^- or O_2-, resulting in a reduced concentration of free electrons at the surface and the observed reduction in the conductivity.

As the temperature is increased, more electrons have sufficient energy to surmount the barrier height between the grains. It can be observed that there is a decrease in the measured current as the temperature is further raised above 300 °C indicating an increase in the film's resistance. This effect is observed in the chemisorption region at elevated temperatures (200 – 400 °C).

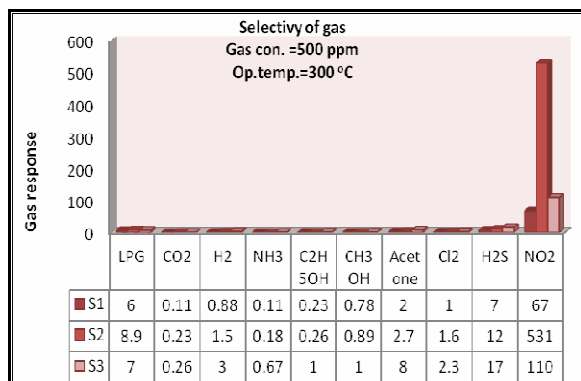### 3.6.2. Selectivity of NO$_2$ for V$_2$O$_5$ thin films for various gases

	LPG	CO2	H2	NH3	C2H5OH	CH3OH	Acetone	Cl2	H2S	NO2
S1	6	0.11	0.88	0.11	0.23	0.78	2	1	7	67
S2	8.9	0.23	1.5	0.18	0.26	0.89	2.7	1.6	12	531
S3	7	0.26	3	0.67	1	1	8	2.3	17	110

Figure 10. Selectivity of nanostructured V$_2$O$_5$ thin films for different gases.

Selectivity can be defined as the ability of a sensor to respond to a certain gas in the presence of other gases [22]. Fig.10 shows the histogram of the selectivity of V$_2$O$_5$ thin films to various gases. The sensing properties of the prepared nanostructured V$_2$O$_5$ thin films for different gases like LPG, CO$_2$, H$_2$, NH$_3$, C$_2$H$_5$OH, Cl$_2$ etc was also investigated at different operating temperature (As shown in Fig. 10).It is observed that the nanorod V$_2$O$_5$ thin films sensor elements was shown poor response to other gases. Thus the Figure 10 shows selectivity of S1, S2 and S3 thin films to NO$_2$ against LPG, CO$_2$, H$_2$, NH$_3$, C$_2$H$_5$OH and Cl$_2$ gases at 350 ^{O}C.

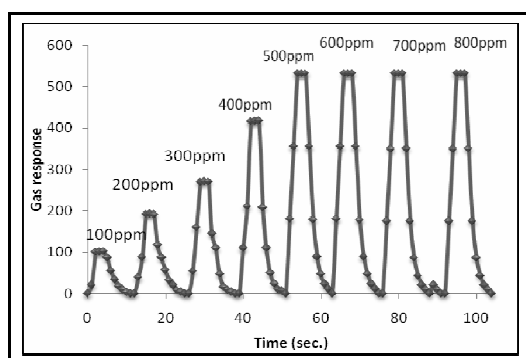### 3.6.3. Response and recovery of the sensor

Figure 11. Response and recovery with concentration of gas (ppm) of the sensor.

Response and recovery time were the basic parameters of the gas sensors. The response time was defined as the time taken for sensor to attain 90 % of maximum change in resistance or conductance upon exposure to NO$_2$. The time taken by the sensors to get back 90 % of original resistance or conductance is the recovery time [23].

The response and recovery of the nanostructured V$_2$O$_5$ thin film (S2) sensor on exposure of 500 ppm of NO$_2$ at 350°C are represented in Fig. 11.The response is quick (2 s) and recovery is fast (11 s). The high oxidizing ability of adsorbed oxygen species on the surface nanoparticles and high volatility of desorbed by-products explain the quick response to NO$_2$ and fast recovery. It can be observed that the sensor sensitivity increased when exposed to NO$_2$ with higher concentration levels, as shown in Figure 11, which revealed to change of sensitivity with concentration of gas.

4. Discussion

4.1. Gas sensing mechanism

As an oxidizing gas with electron affinity much higher than oxygen, NO$_2$ can interact with V$_2$O$_5$ by trapping electrons directly and/or through the surface oxygen ions once it is adsorbed on the V$_2$O$_5$ surface,

namely direct electron-trapping and indirect electron-trapping, respectively, thereby forming new surface electron acceptor levels (Fig. 12b) [24–26].
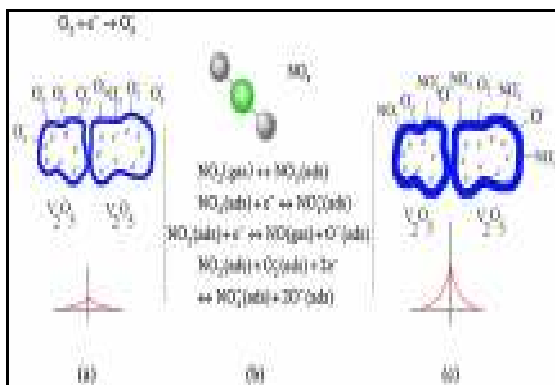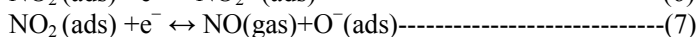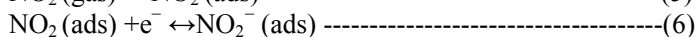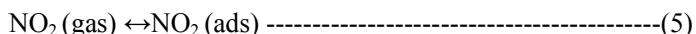
NO_2 (gas) $\leftrightarrow NO_2$ (ads) --(5)
NO_2 (ads) $+e^- \leftrightarrow NO_2^-$ (ads) -------------------------------------(6)
NO_2 (ads) $+e^- \leftrightarrow NO(gas)+O^-$ (ads)-----------------------------(7)
NO_2 (ads) $+O_2^-$ (ads) $+2e^- \leftrightarrow NO_2^-$ (ads)$+2O^-$ (ads))--------(8)

Figure 12. Schematic illustration of the NO_2 sensing mechanism of V_2O_5 sensors.

It should be noted that the reaction path in (5)–(8) is, however, not necessarily the real one, mainly in the presence of the humidity, but it is frequently utilized in quantitative modeling [27]. According to the in-depth theoretical calculation on the expected sensor response functions of n-type semiconducting oxides for NO_2 by Bari et al. [28], the exponent values depend on the final adsorbed species at the surface: when the adsorbed species are NO_2^- or O^-.

5.Conclusions

In this paper the effect of structure, morphology and electrical is explained and discussed. These properties have stimulated considerable research and development interest for their application in recent year. Nanostructured V_2O_5 thin films could be prepared by simple and inexpensive spray pyrolysis technique.The XRD spectra showed that the V_2O_5 have been monoclinic phase with nanostructured in nature. FE-SEM studies revealed a uniform structure of V_2O_5.From XRD and FE-SEM grains size were increases with increase in film thickness. While the activation energy was decreases.Increase in the conductivity with the increase in temperature indicated the semiconducting nature of nanostructured V_2O_5 thin films.The operating temperature was found to be 350 ^{0}C. Maximum sensor sensitivity was found to be 531 for 500 ppm of gas concentration and saturated thereafter.Gas sensing dependent on grain size, grain boundary, nature of gas, operating temperature, crystalline size, Surface area, surface to volume ratio, potential barrier height etc. The nanostructured V_2O_5 thin films exhibit rapid response–recovery which is one of the main features of this sensor.

Acknowledgements

References:

1. Y.Y. Wu, H.Q. Yan, M. Huang, B. Messer, J.H. Song and P.D. Yang, Inorganic nanowires Rational growth, assembly and novel properties, Chem. Eur. J., 2002, 8, 1261-1268.
2. Z.W. Pan, Z. R. Dai and Z.L. Wang, Nanobelts of semiconducting oxides, Science, 2001, 291, 1947-1949.
3. Y.N. Xia, P.D. Yang, Y.G. Sun, Y.Y. Wu, B. May-ers, B. Gates, Y.D. Yin, F. Kim and H.Q. Yan, One-dimensional nanostructures: synthesis, characterization, and applications, Adv.Mater., 2003, 15, 353-389.

4. S.M.A. Durrani, E.E. Khawaja, M.F. Al-Kuhaili, CO-sensing properties of undoped and doped tin oxide thin films prepared by electron beam evaporation, Talanta, 2005, 65, 1162–1167.
5. O. Wurzinger, G. Reinhardt, CO-sensing properties of doped SnO_2 sensors in H_2-rich gases, Sensors and Actuators B, 2004, 103 104–110.
6. M. de la L. Olvera, R. Asomoza, SnO_2 and SnO_2:Pt thin films used as gas sensors, Sensors and Actuators B, 1997, 45, 49–53.
7. K. Murakami, K. Nakajima, S. Kaneko, Initial growth of SnO_2 thin film on the glass substrate deposited by the spray pyrolysis technique, Thin Solid Films, 2007, 515, 8632-8636.
8. T. Mochida, K. Kikuchi, T. Kondo, H. Ueno, Y. Matsuura, Highly sensitive and selective H_2S gas sensor from r.f. sputtered SnO_2, thin film, Sens. Actuators B, 1995, 24, 433–437.
9. D. Vasanth Raj, N. Ponpandian, D. Mangalaraj, C. Viswanathan, Effect of annealing and electrochemical properties of sol–gel dip coated nanocrystalline V_2O_5 thin films, Materials Science in Semiconductor Processing,2012(Article in Press).
10. in-Kyu Lee, Gil-Pyo Kim, In Kyu Song, Sung-Hyeon Baeck, Electrodeposition of mesoporous V_2O_5 with enhanced lithium-ion intercalation property, Electrochemistry Communications, 2009, 11, 1571-1574.
11. S.Shi,M.Cao,X.He,H.Xie, Crystal Growth & Design, 2007,7, 1893–1897.
12. C.D.Guerra,J.Piqueras,Crystal Growth & Design,2008,8,1031–1034.
13. C. V. Ramana, R. J. Smith, O. M. Hussain, M. Massot and C. M. Julien, Surface analysis of pulsed laser-deposited V_2O_5 thin films and their lithium intercalated products studied by Raman spectroscopy, Surface and interface analysis, 2005, 37, 406–411.
14. Youichi Shimizu, Katsumi Nagase, Norio Miura and Noboru Yamazoe, New Preparation process of V_2O_5 thin film based on spin-coating from organic vanadium solution, Jap. J. Appl. Phys., 1990, 29, L1708.
15. W. M. Sears and M. A. Gee, Mechanics of film formation during the spray pyrolysis of tin oxide, Thin Solid Films, 1998, 165, 265-277.
16. ASTM card no.00-054-0513.
17. C.W.Zou,X.D.Yan,J.Han,R.Q.Chen,W.Gao, Microstructures and optical properties of β-V_2O_5 nanorods prepared by magnetron sputtering, Journal of Physics D: Applied Physics,2009, 42,145402.
18. V. B. Patil, G. S. Shahane and L. P. Deshmukh, Studies on photoelectrochemical (PEC) cells; A correlation between electrochemical and material properties, Materials Chemistry and Physics, 2003, 80, 625-632.
19. K.C. Sharma, J.C. Garg, Influence of thermal annealing in air on the electrooptic characteristic of chemical bath deposited non-stoichiometric cadmium zinc selenide thin films, Phys. D: Appl. Phys, 1990, 23, 1411–1419.
20. Z.S. EL-Mandouh, M. EL-Shabasy, Transport properties of $(PbTe)_{9.7}Sb_{0.3}$ thin films, FIZIKA,1995, A4,17–31.
21. L.A. Patil, A.R. Bari, M.D. Shinde, V. D. Deo, Ultrasonically prepared nanocrystalline ZnO thin films for highly sensitive LPG sensing, Sensors and Actuators B: Chemical, 2010,149, 79-86.
22. R. H. Bari, S. B .Patil, A.R. Bari, G .E. Patil, J. Aambekar, Spray pyrolysed nanostructured ZnO thin film sensors for ethanol gas, Sensors & Transducers Journal, 2012,140,124-132.
23. G. H. Jain, L. A. Patil, M. S. Wagh, D. R. Patil, S. A. Patil, D. P. Amalnerkar, Surface modified $BaTiO_3$ thick film resistors as H_2S gas sensors, Sensors and Actuators B: Chemical,2006,117,159-165.
24. Huan Liu, Jiuxiao Wan, Qiuyun Fu, Min Li, Wei Luo, Zhiping Zheng, Hefeng Cao,Yunxiang Hu, Dongxiang Zhou, Tin oxide films for nitrogen dioxide gas detection at low temperatures, Sensors and Actuators B,2013, 177, 460– 466.
25. B. Ruhland, Th. Becker, G. Muller, Gas-kinetic interactions of nitrous oxides with SnO_2 surfaces, Sensors and Actuators B,1998, 50, 85–94.
26. M. Epifani, J.D. Prades, E. Comini, E. Pellicer, M. Avella, P. Siciliano, G. Faglia, A. Cirera, R. Scotti, F. Morazzoni, J.R. Morante, The role of surface oxygen vacancies in the NO_2 sensing properties of SnO_2 nanocrystals, Journal of Physical Chemistry C,2008, 112,19540–19546.
27. A. Oprea, N. Barsan, U. Weimar, Work function changes in gas sensitive materials: fundamentals and applications, Sensors and Actuators B,2009, 142, 470–493.
28. R. H. Bari, S. B. Patil, Low temperature NO_2 sensing performance of nanostructured SnO_2 thin films, Archives of Physics Research, 2014, 5, 1-11.

✱✱✱✱✱